# Tailoring the Ultrathin Al-Induced Crystallization Temperature of Amorphous Si by Application of Interface Thermodynamics

Z. M. Wang, J. Y. Wang,* L. P. H. Jeurgens, and E. J. Mittemeijer

*Max Planck Institute for Metals Research, Heisenbergstrasse 3, D-70569 Stuttgart, Germany*

(Received 11 July 2007; published 27 March 2008)

It has been demonstrated theoretically and experimentally that the thickness of a very thin, pure Al film put on top of an amorphous Si (*a*-Si) layer can be used as a very accurate tool to control the crystallization temperature of *a*-Si. The effect has been explained quantitatively by application of surface-interface thermodynamics. The predictions have been confirmed experimentally by a real-time *in situ* spectroscopic ellipsometry investigation of the crystallization temperature of *a*-Si as a function of the thickness of ultrathin Al layers.

DOI: 10.1103/PhysRevLett.100.125503 PACS numbers: 61.43.Dq, 05.70.Np, 07.60.Fs, 81.10.Aj

The technological demand to produce thin, well-defined crystalline Si (*c*-Si) films, for application in, e.g., liquid crystal displays, organic light emitting devices and solar cells, has led to keen interest in metal-induced crystallization (MIC) of amorphous Si (*a*-Si) films in nanoelectronic devices (cf. Refs. [1–12]). In MIC, the temperature for crystallization of *a*-Si can be greatly reduced if it is put in direct contact with a metal such as Al, Ni, or Au. For example, for *a*-Si in contact with Al the crystallization temperature ($T^{\mathrm{cryst}}$) can be as low as 165 °C [7], as compared with the $T^{\mathrm{cryst}}$ of bulk *a*-Si of about 650 °C [2]. Up until the present, a fundamental understanding of this effect, such that it can be applied to control the $T^{\mathrm{cryst}}$, has not been achieved, which has been due to limited fundamental and comprehensive knowledge on the thermodynamics of the MIC process as a function of the annealing conditions, the layer sequence, and the type and thickness of the "catalytic" metal film.

In the present work, it is demonstrated theoretically and confirmed experimentally that the thickness of a very thin ($< 20$ nm), pure Al film put on top of an *a*-Si layer can be used as a very accurate tool to tune the $T^{\mathrm{cryst}}$ of *a*-Si. In previous studies on the MIC process in *a*-Si/Al systems (cf. Refs. [2,4–9]), much thicker Al layers were employed to induce the crystallization of *a*-Si at low temperatures, which, to date, has obstructed the striking observation of the dependence of the $T^{\mathrm{cryst}}$ of *a*-Si on the Al sublayer thickness (as observed and quantitatively described in the present Letter). On the basis of thermodynamic model calculations, which account for the crucial role of surface and interface energetics, it is shown that the $T^{\mathrm{cryst}}$ of *a*-Si decreases from about 700 °C to 200 °C for an increase of the thickness $h_{\mathrm{Al}}$ of the covering Al film from $h_{\mathrm{Al}} < 1$ nm to $h_{\mathrm{Al}} = 20$ nm. This model prediction is confirmed by investigation of the $T^{\mathrm{cryst}}$ of *a*-Si as a function of the Al film thickness in the range of 0.7–20 nm using real-time *in situ* spectroscopic ellipsometry (RISE). This contribution not only provides pronounced fundamental insights into the process of metal-induced crystallization, but also demonstrates in general how surface and interface energetics (as modeled here on the basis of the so-called macroscopic atom approach [13]) control diffusion, wetting, and phase transformations in low-dimensional systems. Moreover, pronounced technological progress in the low-temperature manufacturing of *c*-Si-based, nanoelectronic devices may be expected as a result of this work.

Two mechanisms have been postulated to explain the observation of the Al-induced crystallization (AIC) of *a*-Si layers at temperatures well below the $T^{\mathrm{cryst}}$ of bulk *a*-Si: (i) AIC would be mediated by the formation of a metastable Al silicide phase at the Al/*a*-Si interface as an intermediate state [10–12] and (ii) AIC would be the result of the nucleation and growth of *c*-Si at favorable sites at the Si/Al interface and/or within the Al layer [e.g., at the Al grain boundaries (GBs)] [1,4–9]. An *in situ* high-resolution transmission electron microscopic (HRTEM) study on annealed *a*-Si/*c*-Al multilayers has provided direct experimental evidence for the nucleation of single-phase *c*-Si at Al GBs [1] (i.e., without the intermediate formation of a mixed Al/Si or silicide phase). For an Al layer without GBs or with negligible GB density, no Al-induced crystallization of *a*-Si can be observed [8]. Corresponding differential scanning calorimetry (DSC) and x-ray diffraction (XRD) measurements also rule out the formation of a metastable silicide phase upon metal-induced crystallization in the *a*-Si/*c*-Al system [1,2,6–9]. This contrasts with the experimental observations in the *a*-Si/*c*-Au system: i.e., the formation of a metastable Au-silicide (and its *lateral* growth) at Au GBs has been directly observed by HRTEM [3], DSC and XRD [3,14], which is also in accordance with recent thermodynamic model predictions for this system [9].

Against the above background, the idea for the present project emerged; see the sketch in Fig. 1(a). As a result of the so-called screening effect [15], the Coulomb interaction between the Al metal phase and the adjacent *a*-Si phase leads to the weakening of the covalent bonds in a very thin interfacial region of the *a*-Si phase (thickness of 2 monolayers (ML) [16], where 1 ML Si = 0.22 nm [17]) in contact with the Al metal, thereby allowing an enhanced

 © 2008 The American Physical Society

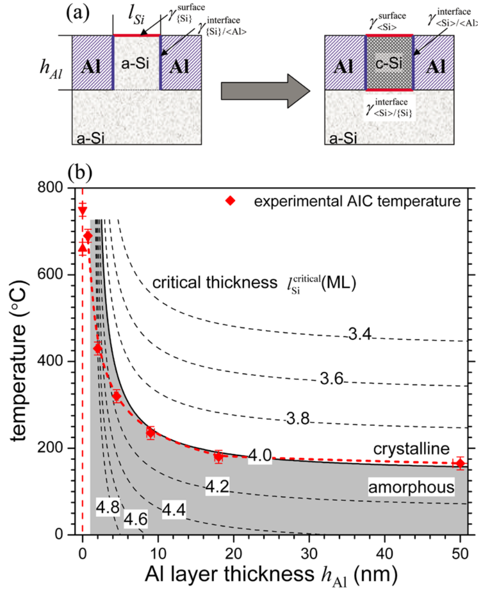


FIG. 1 (color online). (a) Schematic representation of the thermodynamic model for the initiation of crystallization of *a*-Si at Al GBs in the ultrathin, columnar Al overlayer of thickness $h_{Al}$, recognizing that $h_{Al}$ is comparable with the thickness of the Al GB wetting layer of *a*-Si, $l_{Si}$. (b) Calculated critical thickness for initiation of crystallization of *a*-Si at Al GBs ($l_{Si}^{critical}$) as function of both Al layer thickness $h_{Al}$ and temperature. The experimental results for the dependence of AIC temperature on $h_{Al}$ attained in the present work have been indicated. The point corresponding to Al layer thickness of 50 nm has been taken from Ref. [7].

mobility for interface-adjacent "free" Si atoms. These free Si atoms can diffuse into GBs of the adjacent Al phase because a thermodynamic driving force for this GB wetting process exists [8]. The wetting *a*-Si layer at the Al GBs is sandwiched between two *c*-Al grains and therefore the thickness $l_{Si}$ of the wetting *a*-Si layer is smaller than or maximally equal to $2 \times 2 = 4$ ML. This weakly bonded *a*-Si wetting layer may be the agent for the initiation of crystallization of *a*-Si at low temperatures (see below). Since the formation of an intermediate (metastable) Al silicide phase upon MIC in the *a*-Si/*c*-Al system can be ruled out (see above), it follows that the initiation of MIC in this system thus involves the transport of *only* Si (and not of Al).

For comparably small values of the Al layer thickness, $h_{Al}$, and taking the Al GB as oriented more or less perpendicular to the surface [7], it follows that upon initiation of crystallization of the wetting *a*-Si film at the Al GBs [1], (i) not only the *interfacial* energy change [per unit length along the Al GB parallel to the surface; i.e., perpendicular to the plane of drawing in Fig. 1(a)], $2h_{Al}(\gamma^{interface}_{\langle Si\rangle/\langle Al\rangle} - \gamma^{interface}_{\{Si\}/\langle Al\rangle})$, associated with the replacement of the two original *amorphous*-crystalline $\{Si\}/\langle Al\rangle$ interfaces by two *crystalline*-crystalline $\langle Si\rangle/\langle Al\rangle$ interfaces, but (ii) also the surface and interfacial energy changes (per unit length along the Al GB parallel to the surface) $l_{Si}(\gamma^{surface}_{\langle Si\rangle} - \gamma^{surface}_{\{Si\}})$ and $l_{Si}\gamma^{interface}_{\langle Si\rangle/\{Si\}}$, due to the formation of the crystalline $\langle Si\rangle$ surface and the crystalline/amorphous $\langle Si\rangle/\{Si\}$ interface, respectively, have to be considered [see Fig. 1(a)]. Note that the amorphous and crystalline phases are denoted by braces {} and brackets ⟨⟩, respectively.

Crystallization of the wetting *a*-Si layer at the Al GBs is favored by bulk thermodynamics (due to the lower Gibbs energy of bulk *c*-Si as compared to that of *a*-Si, as given by the crystallization energy, $\Delta G^{crystallization}_{\langle Si\rangle\text{-}\{Si\}}$, per unit volume), but opposed by the associated increases of the surface and interface energies caused by the crystallization [see Fig. 1(a), and further below]. The change in the total Gibbs energy, $\Delta G^{total}$, of the considered *a*-Si/Al system upon crystallization of the thin wetting *a*-Si layer (per unit length along the Al GB parallel to the surface) is given by:

$$\Delta G^{total} = l_{Si}h_{Al}\Delta G^{crystallization}_{\langle Si\rangle-\{Si\}}(T) + 2h_{Al}[\gamma^{interface}_{\langle Si\rangle/\langle Al\rangle}(T) - \gamma^{interface}_{\{Si\}/\langle Al\rangle}(T)] + l_{Si}\{[\gamma^{surface}_{\langle Si\rangle}(T) - \gamma^{surface}_{\{Si\}}(T)] + \gamma^{interface}_{\langle Si\rangle/\{Si\}}(T)\}. \quad (1)$$

It follows that a critical thickness of the wetting *a*-Si layer, $l_{Si}^{critical}$, for initiation of crystallization of *a*-Si at the Al GBs, can now be determined by balancing the *bulk* crystallization energy with the accompanying increases in *surface* and *interface* energies of the system [i.e., by solving Eq. (1) for $\Delta G^{total} = 0$]

$$l_{Si}^{critical} = \frac{2[\gamma^{interface}_{\langle Si\rangle/\langle Al\rangle}(T) - \gamma^{interface}_{\{Si\}/\langle Al\rangle}(T)]}{-\Delta G^{crystallization}_{\langle Si\rangle-\{Si\}}(T) - \frac{[\gamma^{surface}_{\langle Si\rangle}(T) - \gamma^{surface}_{\{Si\}}(T)] + \gamma^{interface}_{\langle Si\rangle/\{Si\}}(T)}{h_{Al}}}. \quad (2)$$

A method for assessing surface and interface energies in a wide range of crystalline and amorphous materials has been provided [13,18], based on which values for the surface and interface energies involved in the present study can be obtained [9]. It is noted that the decrease in configurational entropy (i.e., an ordering effect [19,20]) in the (bond-weakened) *a*-Si wetting film due to the adjacent crystalline Al metal grains is explicitly accounted for in the calculation of amorphous-crystalline interface energies (see Refs. [9,18] for details). Some typical values of the corresponding energies (i.e., at 200 °C and 400 °C) have been given in Table I. Thus the critical thickness $l_{Si}^{critical}$ can be analyzed quantitatively as function of both $h_{Al}$ and $T$. The results obtained for $l_{Si}^{critical}$ (expressed in units of ML) are shown as a contour-plot in Fig. 1(b) as function of both $h_{Al}$ and $T$. For $T$ between 0 °C and 500 °C and $h_{Al} < 50$ nm, $l_{Si}^{critical}$ typically ranges from ~3.4 ML to ~4.8 ML. $l_{Si}^{critical}$ strongly depends on $T$ and decreases with increasing $T$ at fixed $h_{Al}$. A strong dependence of $l_{Si}^{critical}$ on $h_{Al}$ occurs particularly for $h_{Al} < 20$ nm: $l_{Si}^{critical}$ increases strongly with decreasing $h_{Al}$ (<20 nm). For thicker Al layers ($h_{Al} > 30$ nm), $l_{Si}^{critical}$ is almost solely determined by $T$.

The bond-weakening effect involves that the wetting $a$-Si layer has a maximum thickness of 4 ML (cf. above discussion). Hence, $l_{\mathrm{Si}}^{\mathrm{critical}}$ must be smaller than (or maximally equal to) 4 ML in order that crystallization is possible. This maximum value for the critical thickness $l_{\mathrm{Si}}^{\mathrm{critical}}$ of 4 ML has been indicated by the solid line in Fig. 1(b). A critical thickness smaller than 4 ML implies that crystallization can occur, whereas a critical thickness larger than 4 ML implies that the $a$-Si phase in the system stays amorphous. Thus amorphous and crystalline zones can be indicated in Fig. 1(b). Hence, the thermodynamic prediction of the $T^{\mathrm{cryst}}$ of $a$-Si as function of $h_{\mathrm{Al}}$ is given by the solid line $l_{\mathrm{Si}}^{\mathrm{critical}} = 4$ ML in Fig. 1(b). It follows that the $T^{\mathrm{cryst}}$ is around 150–200 °C for $h_{\mathrm{Al}} > 20$ nm. For $h_{\mathrm{Al}} <$ 20 nm, the $T^{\mathrm{cryst}}$ increases rapidly with decreasing $h_{\mathrm{Al}}$.

To verify the above thermodynamic prediction experimentally, an investigation of the onset $T^{\mathrm{cryst}}$ of $a$-Si in $\mathrm{Al}/a-\mathrm{Si}$ bilayers with various Al overlayer thicknesses by an *in situ* real-time technique is required. The annealing process must be carried out in ultrahigh vacuum (UHV) due to the very high reactivity of Al with oxygen. The formation of Al oxide would change the thickness of the Al overlayer, and also the surface energetics of the system and therefore invalidate a reliable comparison between experimental results and theoretical predictions. Therefore, in this study, RISE in UHV has been applied which has been shown to be extremely sensitive to changes in local order in Si by monitoring the microstructural evolution of Si films with thicknesses as small as 1 nm [21–24].

The $a$-Si thin films (thickness values between 38 and 40 nm) and the Al overlayers (thickness: 0.7–18 nm) were grown onto a degassed 15-nm $\mathrm{SiO_2/Si}$ substrate sequentially by evaporation in an UHV multisource molecular beam epitaxy system (base pressure $<1.5 \times 10^{-10}$ mbar, Si, Al purity $>99.999$ at.%). The specimen holder was cooled by water to keep the substrate at a low temperature during film growth. The thicknesses of the $a$-Si and Al layers were determined at room temperature by *in vacuo* spectroscopic ellipsometry. The $\mathrm{Al}/a$-Si bilayer specimens were then heated up slowly (10 °C/ min ) in UHV and the RISE data during heating up were collected using a J. A. Woollam M2000U-XE rotating compensator ellipsometer (wavelength $\lambda = 245$–1000 nm), with a time step of 2.5 s [25].

The optical absorption of amorphous Si shows a broad peak around a photon energy of 3.5 eV [22–24]. This broad absorption peak separates into two sharper prominent structures at about 4.2 and 3.4 eV for crystalline Si [22,24,26]. For application of RISE to the real-time *in situ* monitoring of the crystallization of $a$-Si, the directly measured ellipsometric amplitude-ratio and phase-shift dependent parameters, $\Psi(\lambda)$ and $\Delta(\lambda)$ respectively, were reparametrized as the pseudodielectric function $\varepsilon(E) = \varepsilon_1(E) + i\varepsilon_2(E)$ (with $E$: photon energy) during the *in situ* measurement (see what follows) [24].

The evolutions of pseudo-$\varepsilon_2$ at two photon energies, 2.2 and 4.0 eV, during annealing of a 4.5-nm Al/40-nm $a$-Si specimen, are shown in Fig. 2(a). At both energies a slight increase in pseudo-$\varepsilon_2$ with increasing temperature is observed at temperatures below 320 °C, which corresponds with the temperature dependence of the optical constants [26] and also a possible relaxation and densification process of $a$-Si. At about 320 °C, a pronounced decrease of pseudo-$\varepsilon_2$ at 2.2 eV occurs, associated with a pronounced increase of pseudo-$\varepsilon_2$ at 4.0 eV. The detailed evolution of the pseudo-$\varepsilon_2$ spectrum (i.e. as function of photon energy) during annealing at 320 °C (and above) is shown in the inset of Fig. 2(a). The fast increase in pseudo-$\varepsilon_2$ at photon energies around 4.0 eV clearly indicates the formation of crystalline Si [22]. The simultaneous decrease in pseudo-$\varepsilon_2$ at photon energies around 2.2 eV is not only related to the crystallization of $a$-Si [22], but is also partly ascribed to the inward "movement" of Al upon continued crystallization of the $a$-Si phase (eventually $c$-Al → $c$-Si layer exchange will occur [5,6]), since Al shows strong absorption around 1.6 eV [27]. The concurrent processes of progressing crystallization of the $a$-Si phase and eventually complete $c$-Al → $c$-Si layer exchange have been confirmed by *in vacuo* RHEED analysis and *ex situ* Auger electron spectroscopic depth profiling measurements after annealing (not shown here). It is concluded that the evolution of pseudo-$\varepsilon_2$ for the 4.5-nm Al/40-nm $a$-Si specimen indicates that the crystallization of $a$-Si initiates at 320 °C. An onset temperature of 320 °C for initiation of AIC is therefore determined. Corresponding RISE results for an 18-nm Al/40-nm $a$-Si specimen are shown in Fig. 2(b). It follows that the onset temperature for initiation of AIC is 180 °C, which is much lower than that for the 4.5-nm Al/40-nm $a$-Si specimen. Further, the rapid decrease in absorption (i.e., pseudo-$\varepsilon_2$) around 2 eV clearly indicates the occurrence of layer exchange during crystallization (see inset in Fig. 2(b) and discussion above). Comparing Figs. 2(a) and 2(b), it follows that a thicker Al overlayer results in faster crystallization of the $a$-Si phase, albeit the $T^{\mathrm{cryst}}$ is lower. This kinetic difference may be ascribed to a larger total GB area

TABLE I. Values of the crystallization, surface and interface energies in the Al/Si layer system at typical temperatures of 200 °C and 400 °C, as calculated according to Refs. [9,13,18].

| Temperature(°C) | $\Delta G_{\langle\mathrm{Si}\rangle\text{-}\{\mathrm{Si}\}}^{\mathrm{crystallization}}$ (J/m$^3$) | $\gamma_{\langle\mathrm{Si}\rangle}^{\mathrm{surface}}$ (J/m$^2$) | $\gamma_{\{\mathrm{Si}\}}^{\mathrm{surface}}$ (J/m$^2$) | $\gamma_{\langle\mathrm{Si}\rangle/\langle\mathrm{Al}\rangle}^{\mathrm{interface}}$ (J/m$^2$) | $\gamma_{\{\mathrm{Si}\}/\langle\mathrm{Al}\rangle}^{\mathrm{interface}}$ (J/m$^2$) | $\gamma_{\langle\mathrm{Si}\rangle/\{\mathrm{Si}\}}^{\mathrm{interface}}$ (J/m$^2$) |
|---|---|---|---|---|---|---|
| 200 | $-8.9 \times 10^8$ | 1.37 | 0.98 | 0.45 | 0.07 | 0.08 |
| 400 | $-8.4 \times 10^8$ | 1.35 | 0.96 | 0.42 | 0.10 | 0.10 |

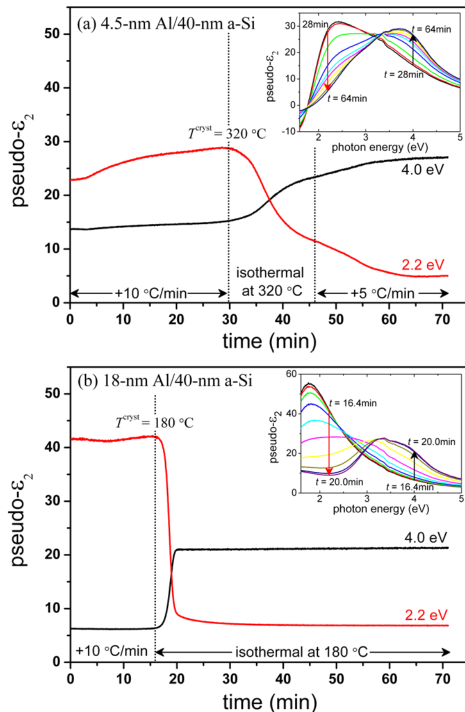


FIG. 2 (color online). (a) Real-time evolutions of the imaginary part $\varepsilon_2$ of the pseudodielectric function of a 4.5-nm Al/40-nm *a*-Si specimen at photon energies of 2.2 and 4.0 eV during annealing. (Inset) The corresponding detailed pseudo-$\varepsilon_2$ spectra (i.e., as function of photon energy) between 1.6 and 5.0 eV for annealing times in the range of 28 to 64 min, corresponding to the AIC process (see discussion in text). (b) Same as (a), for an 18-nm Al/40-nm *a*-Si specimen.

available for nucleation of Si crystallization in the thicker Al layer.

The thus measured onset AIC temperatures as a function of Al overlayer thickness, based on RISE measurements of a series of Al/*a*-Si specimens (Al thickness: 0.7, 2, 4.5, 9, and 18 nm), have been indicated in Fig. 1(b). Furthermore, the onset $T^{\text{cryst}}$ of two pure 40-nm *a*-Si specimens, prepared and measured as described above, one with a clean surface, and the other one with a thin oxide passivation layer, have also been indicated in Fig. 1(b), at $h_{\text{Al}} = 0$ nm as up- and down-ward triangles, respectively. It follows that the experimental $T^{\text{cryst}}$ not only reproduce the thermodynamically predicted dependence of the onset value of $T^{\text{cryst}}$ on the Al layer thickness, but also agree very well quantitatively with the model-calculated locus for the critical thickness at about 4.0 ML in Fig. 1(b). For $h_{\text{Al}}$ values smaller than 4.5 nm, the $T^{\text{cryst}}$ increases to temperatures at which thermal fluctuations of the Si atoms become that pronounced that an increase can be expected of the thickness of the weakly bonded *a*-Si layer at the Al GBs. Consequently, then the experimental $T^{\text{cryst}}$ becomes lower than that calculated for $l_{\text{Si}}^{\text{critical}} = 4$ ML [see Fig. 1(b)]; thus, for an Al overlayer of 2 nm, the $T^{\text{cryst}}$ is found to be about 440 °C, corresponding to $l_{\text{Si}}^{\text{critical}} = 4.8$ ML. If the Al layer thickness is that thin that no Al GBs may form in the Al "layer", the $T^{\text{cryst}}$ will be as high as the one for crystallization of pure *a*-Si. This has been demonstrated by experimental results obtained for $h_{\text{Al}} = 0.7$ nm with a $T^{\text{cryst}}$ of 690 °C.

The presented thermodynamic model calculations and corresponding experimental validation provide a fundamental and comprehensive understanding of the process of ultrathin Al-induced crystallization of *a*-Si, which is exclusively initiated at Al GBs. It follows that this Al GB-mediated crystallization is controlled by *thermodynamics:* balancing *bulk* energy change with *surface and interface* energy changes. As a result, the Al (over)layer thickness can be employed to tailor sensitively the crystallization temperature of *a*-Si in contact with *c*-Al.

*j.y.wang@mf.mpg.de

[1] T. J. Konno and R. Sinclair, Philos. Mag. B **66**, 749 (1992).
[2] T. J. Konno and R. Sinclair, Mater. Sci. Eng. A **179**, 426 (1994).
[3] M. Seibt *et al.*, Phys. Rev. Lett. **80**, 774 (1998).
[4] O. Nast and A. J. Hartmann, J. Appl. Phys. **88**, 716 (2000).
[5] O. Nast and S. R. Wenham, J. Appl. Phys. **88**, 124 (2000).
[6] Y. H. Zhao, J. Y. Wang, and E. J. Mittemeijer, Appl. Phys. A **79**, 681 (2004).
[7] D. He, J. Y. Wang, and E. J. Mittemeijer, J. Appl. Phys. **97**, 093524 (2005).
[8] J. Y. Wang *et al.*, Appl. Phys. Lett. **88**, 061910 (2006).
[9] Z. M. Wang *et al.*, Phys. Rev. B **77**, 045424 (2008).
[10] M. Yuichi *et al.*, J. Appl. Phys. **76**, 5225 (1994).
[11] P. D. Tilo, B. Jurgen, and G. Hubert, Appl. Phys. Lett. **72**, 1510 (1998).
[12] Y.-C. Her and C.-W. Chen, J. Appl. Phys. **101**, 043518 (2007).
[13] R. Benedictus, A. Böttger, and E. J. Mittemeijer, Phys. Rev. B **54**, 9109 (1996).
[14] R. R. Chromik *et al.*, J. Appl. Phys. **91**, 8992 (2002).
[15] A. Hiraki, Surf. Sci. Rep. **3**, 357 (1984).
[16] Estimated from the photoemission spectroscopic data in H. J. Wen *et al.*, J. Vac. Sci. Technol. A **13**, 2399 (1995).
[17] J. C. Slater, J. Chem. Phys. **41**, 3199 (1964).
[18] F. Sommer, R. N. Singh, and E. J. Mittemeijer, J. Alloys Compd. (to be published).
[19] N. I. Borgardt *et al.*, Phys. Rev. B **70**, 195307 (2004).
[20] S. H. Oh *et al.*, Science **310**, 661 (2005).
[21] I. An *et al.*, Phys. Rev. Lett. **65**, 2274 (1990).
[22] H. V. Nguyen *et al.*, Phys. Rev. Lett. **74**, 3880 (1995).
[23] S. Hazra *et al.*, Phys. Rev. B **69**, 235204 (2004).
[24] W. T. Charles *et al.*, J. Appl. Phys. **97**, 103536 (2005).
[25] M. S. Vinodh, L. P. H. Jeurgens, and E. J. Mittemeijer, J. Appl. Phys. **100**, 044903 (2006).
[26] P. Lautenschlager *et al.*, Phys. Rev. B **36**, 4821 (1987).
[27] H. V. Nguyen, I. An, and R. W. Collins, Phys. Rev. B **47**, 3947 (1993).